Received: 24 July 2018 | Revised: 11 October 2018 | Accepted: 11 October 2018

DOI: 10.1002/eqe.3135

RESEARCH ARTICLE

WILEY

Probabilistic models for structures with bilinear demand-intensity relationships

Gerard J. O'Reilly | Ricardo Monteiro

Scuola Universitaria Superiore IUSS, Pavia, Italy

Correspondence
Gerard J. O'Reilly, Scuola Universitaria Superiore IUSS, Pavia, Italy.
Email: gerard.oreilly@iusspavia.it

Funding information
Italian Ministry of Education, University and Research

Summary

An extension to the existing SAC/FEMA expressions to estimate mean annual frequency of exceedance (MAFE) for a given limit state is described. In specific, this study pertains to structural systems whose demand versus seismic intensity relationship cannot be reasonably represented by a linear fit in logspace, but rather a bilinear fit over the entire range of structural response. Using a predefined limiting intensity, the median demand is separated into two distinct zones of response. These expressions are derived using a second-order polynomial hazard model fit and can be considered a further extension of the closed-form expressions available in the literature. The steps in the derivation are described along with an example application of the proposed expressions. Comparing different models shows that the MAFE can be significantly misrepresented when using a linear demand-intensity model for systems whose behaviour deviates from this assumption in logspace. Similarly, a logarithmic function demand-intensity fit is examined and seen not to be suitable in the specific situations focused on here. Furthermore, significant underestimation or overestimation is observed when using local fits in the vicinity of the behaviour transition point, which highlights the need for such a bilinear model when assessing the structural performance at the transition point's vicinity. Adopting a bilinear model is shown to better represent structural systems with complex response characteristics, also allowing the use of a single demand model for the entire range of response. This is at the same time still compatible with the existing framework for performance-based seismic design and assessment.

KEYWORDS

demand-intensity, probabilistic assessment, reliability, SAC/FEMA, seismic performance

1 | INTRODUCTION

Over the past number of decades, the notion of performance-based seismic design and assessment has evolved from qualitative definitions of structural performance that engineers were aiming to achieve for certain levels of shaking to a fully probabilistic framework. The former aspects stemmed from the advancements outlined in the Vision 2000 document in 1995,[1] whereas the latter aspects, regarding a more probabilistic-oriented approach, were set forth by Cornell and Krawinkler[2] in 2000 through what became commonly known as the Pacific Earthquake Engineering Center (PEER)

performance-based earthquake engineering (PBEE) framework. Whilst probabilistic aspects have been present in the field of earthquake engineering long before the turn of the millennium, their practical implementation to structures was significantly developed during this period. This was culminated through the publication of what became known as the SAC/FEMA methodology by Cornell et al[3] and Jalayer,[4] whereby the performance of a structure, expressed as the mean annual frequency of exceeding (MAFE) a limit state, could be expressed in a fully probabilistic and closed-form solution. It foresaw a number of simplifying assumptions regarding the definition of seismic hazard and the relationship between the structural demand and seismic intensity to arrive at a fully integrated solution in a rather succinct and practical format. This is perhaps best reflected in the implementations of the framework over the years within various analysis methods intended for practical implementation.[5-10]

Since its introduction in 2002, a notable advancement was made to the SAC/FEMA framework in 2013 by both Vamvatsikos[11] and Romão et al,[12] where the linear hazard model in logspace assumption adopted by Cornell et al[3] was extended to a second-order polynomial in logspace in order to better represent the curvature of the seismic hazard curve. This extension of the original framework meant that the basic expressions to estimate the MAFE were derived once again in a similar fashion to those outlined by Jalayer.[4] However, whilst some progress has been made in extending the seismic hazard model representation, the assumption regarding the relationship characterising the median structural demand with increasing seismic intensity (herein referred to as a demand-intensity model) has remained relatively consistent in its formulation and application. This definition of the demand-intensity model essentially centres around the assumption that when transformed to logspace, it can be relatively well defined in the region of interest using a local linear relationship. Jalayer[4] outlines how a simple functional form was sought to relate the storey drift in a structure with increasing intensity that helped simplify analytical efforts in the development of a closed-form solution but also conformed to the physical reasoning one would expect in such a relationship. Analysis methods such as incremental dynamic analysis (IDA)[13] or cloud-type analysis[4] may be used to quantify this relationship between the structural demand and seismic intensity using sets of ground motions to obtain the probabilistic quantification of response directly. Alternatively, more simplified methods such as displacement-based assessment[14] may be used to quantify the median structural response followed by some empirical assumption regarding dispersion.

Whilst this linear demand-intensity relationship in logspace represents a rather convenient format, the use of a unique global fit may not be appropriate over the entire range of structural response for certain structural typologies and demand parameters. This is because the demand-intensity relationship representation in logspace was initially developed assuming that the region of interest could be adequately represented as linear, meaning that for instances where the entire demand-intensity relationship violates this assumption, numerous local fits may be utilised instead for an equally valid implementation (eg, Vamvatsikos and Cornell[13]). This has the disadvantage of requiring many local fits to be established and has tended to result in the actual application of this relationship being so that a single global fit may, sometimes erroneously, be used over the entire demand-intensity range of interest. Therefore, a distinction between global and local fits to the demand-intensity relationship is made.

For example, Romão et al[12] noted how a global linear fit was particularly suited to deformation-based demand parameters like storey drift but rather limited when examining the evolution of force-based parameters like shear force. Romão et al[12] subsequently developed a new logarithmic functional global fit to better represent these force-based parameters over the entire range of response. Additionally, other studies[15,16] have shown that the force-based demands, such as stresses in capacity-designed components, also tend to saturate with increasing intensity as they approach their designated failure modes, meaning that a unique global linear fit is also no longer representative. This limitation of global fits has been noted to occur in situations where two distinct zones of structural behaviour can be identified, whereby the dynamic behaviour with respect to increasing intensity significantly differs, as illustrated in Figure 1. For example, O'Reilly[17] showed how the demand-intensity relationship between maximum peak storey drift (MPSD) along the building height and first-mode spectral acceleration, $Sa(T_1)$, in nonductile RC frames with masonry infill exhibited two distinct response zones similar to that illustrated in Figure 1. The interface between these two zones of response was identified by O'Reilly[17] to be the storey drift at which the masonry infill at the critical storey collapsed, θ_{lim}, meaning that the strength and stiffness of the building reduced significantly and therefore abruptly modified the subsequent dynamic response characteristics of the frames. Other studies like Ramamoorthy et al,[18] for example, have also noted that the use of a single linear relationship in logspace may not be the most effective way of characterising the demand-intensity relationship of RC frame buildings. Similarly, the relationship between maximum peak floor acceleration (MPFA) along the building height and $Sa(T_1)$ has been shown to exhibit two separate response zones, whereby the MPFA tends to saturate with increasing intensity.[19] This can be explained by the simple fact that when the structure yields, the amount of dynamic force and subsequently floor acceleration will become capped by the lateral strength

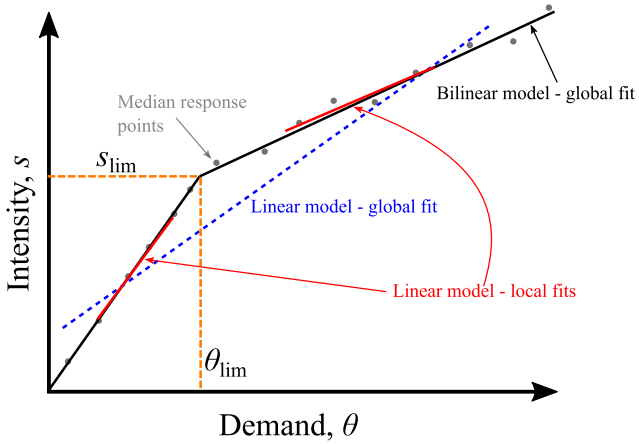

FIGURE 1 Illustration of demand-intensity models where the global linear model misrepresents the median response obtained from analysis, whereas the local linear fits are reasonable in their respective regions and the bilinear model fits well over the entire range of response. Note that the two axes are illustrated in logscale [Colour figure can be viewed at wileyonlinelibrary.com]

of the structure. This means that whilst the seismic intensity increases beyond this limiting intensity, $s_{\lim}$, the MPFA cannot increase beyond a certain level due to the limited lateral strength capacity of the structure. It is noted that some relatively small increases can be expected due to the postyield hardening and contribution of higher modes in taller buildings, but are otherwise noted to be relatively limited. This notion of the structure's yield strength capping the evolution of the demand parameter with respect to increasing intensity was also observed in the work of Romão et al,[12] where the yielding of the structure was noted to limit the shear force with increasing intensity.

Acknowledging the aforementioned limitations of using a single linear fit globally, the linear demand-intensity model assumption is herein extended to a bilinear assumption in logspace whereby a limiting interface is defined based on physical reasoning regarding specific structural systems' response (eg, structural yielding or masonry infill collapse) and the fitting coefficients established for each individual zone of response. It is believed that this segregation of the two zones of response may be considered more consistent with the mechanical behaviour of structures. The functional form and subsequent derivation outlined in Romão et al[12] mean that it is applicable to scenarios where the structural demand tends to be limited beyond a certain threshold, as in the case for MPFA outlined above. However, for the case of the MPSD evolution in infilled RC frames, this formulation would no longer be appropriate since the dependent and independent variables need to be switched to permit the logarithmic function to be utilised. The bilinear extension described herein requires the derivation of the expressions established in the framework outlined by Cornell et al[3] to be repeated in a similar fashion to Jalayer[4] and Vamvatsikos.[11] An example application of these newly proposed expressions is then described to highlight the impacts of different demand-intensity model assumptions when evaluating the performance of pertinent structural systems.

2 | DERIVATION

2.1 | Definition of the problem statement

Seismic hazard can be defined as the mean annual frequency of exceeding the seismic intensity, s, which when adopting the second-order polynomial in logspace, $H(s)$, described by Vamvatsikos,[11] is given by Equation 1:

$$H(s) = k_0 \exp\left[-k_1 \ln s - k_2 \ln^2 s\right] \tag{1}$$

where k_0, k_1, and k_2 are fitting coefficients identified using the output of site hazard analysis. The local rate of exceedance in the range $[s, s + \mathrm{d}s]$ is defined as $-\mathrm{d}H(s)$, where the negative sign is included to account for its decrease with increasing s. Given this rate of a given value of s and knowing the exceedance of a limit state (LS) for a given value of s (ie, a fragility function, as illustrated in Figure 2), then the local rate of LS exceedance, $\mathrm{d}\lambda_{\mathrm{LS}}$, is given by

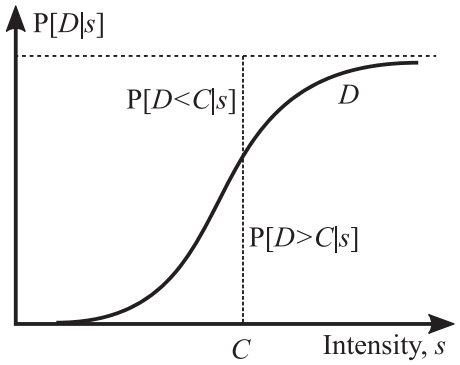

FIGURE 2 Illustration of demand fragility function, D, where the probabilities of exceedance and nonexceedance of the deterministic value of capacity, C, are described by the portions of the vertical below and above the fragility curve, respectively

$$\mathrm{d}\lambda_{\mathrm{LS}}(s) = -P[D > C|s]\mathrm{d}H(s) \tag{2}$$

where D and C denote the demand for a given s and LS capacity, respectively.

The MAFE of LS, λ_{LS}, is found by integrating the local rate for all values of s as follows:

$$\lambda_{\mathrm{LS}} = \int_0^{+\infty} \mathrm{d}\lambda_{\mathrm{LS}}(s) = -\int_0^{+\infty} P[D > C|s]\mathrm{d}H(s) = -\int_0^{+\infty} P[D > C|s]\frac{\mathrm{d}H(s)}{\mathrm{d}s}\mathrm{d}s \tag{3}$$

As described by Jalayer,[4] integration by parts is needed at this point and gives

$$\lambda_{\mathrm{LS}} = -[P[D>C|s]H(s)]_0^{+\infty} + \int_0^{+\infty} \frac{\mathrm{d}P[D > C|s]}{\mathrm{d}s} H(s)\mathrm{d}s \tag{4}$$

The first term can be dropped since the value of $H(\bullet)$ tends to zero at $s = +\infty$, as does the probability at $P\,[D > C|\, s = 0]$, which reduces the result to

$$\lambda_{\mathrm{LS}} = \int_0^{+\infty} \frac{\mathrm{d}P[D > C|s]}{\mathrm{d}s} H(s)\mathrm{d}s \tag{5}$$

and represents the basic format to define the MAFE of a LS.

2.2 | Demand parameter exceedance

The demand parameter, θ, is assumed to be lognormally distributed with a median capacity, $\widehat{\theta}_{\mathrm{C}}$, and an aleatory uncertainty, β_{CR}. The median demand is written as $\widehat{\theta}_{\mathrm{D}}(s)$, as it is a function of seismic intensity, and the associated aleatory uncertainty is denoted β_{DR}, which is assumed to be independent of seismic intensity, or homoscedastic, for mathematical convenience although it is noted that it typically tends to increase in structures for increasing s. The impact of β_{DR}'s dependence on intensity was examined in Aslani and Miranda,[20] for example, who noted that of the assumptions required to implement the closed-form solution for MAFE described in Cornell et al,[3] this had the smallest influence, when compared with the simplifications in demand-intensity model and hazard curve fitting. The handling of dispersion and uncertainty will be addressed further in Section 2.3. For now, the capacity is assumed to be deterministic for simplicity of the derivation (ie, $\beta_{\mathrm{CR}} = 0$) and is thus denoted θ_{C}. It will be later discussed how the expressions developed herein can be extended to a probabilistic definition of the capacity. Assuming lognormality for the demand gives

$$P[D > C|s] = P[\ln\theta_{\mathrm{D}} > \ln\theta_{\mathrm{C}}|s] = 1 - \Phi\left(\frac{\ln\theta_{\mathrm{C}} - \ln\widehat{\theta}_{\mathrm{D}}(s)}{\beta_{\mathrm{DR}}}\right) \tag{6}$$

where $\Phi(\bullet)$ represents the cumulative distribution function (CDF) of a normal distribution (it is noted that when C is considered as deterministic, its probability density function (PDF) reduces to a vertical line at θ_{C}). Substituting Equation 6 into Equation 5 gives

$$\lambda_{LS} = \int_0^{+\infty} \frac{d}{ds}\left[1 - \Phi\left(\frac{\ln\theta_C - \ln\widehat{\theta}_D(s)}{\beta_{DR}}\right)\right] H(s)ds \tag{7}$$

As outlined in Cornell et al,[3] the median demand, $\widehat{\theta}_D$, can be reasonably approximated with respect to s as follows:

$$\widehat{\theta}_D(s) \approx as^b \tag{8}$$

where a and b are coefficients fitted to median structural response obtained via some form of structural analysis. Equation 8 essentially implies that the relationship between the structural demand and seismic intensity can be locally represented as linear in logspace. This holds well for many situations encountered in earthquake engineering, and a single global fit can often be used but is noted to not always hold true for certain structural typologies and/or demand parameters. This aspect is discussed further in Section 4, and the derivation of an expression to estimate LS exceedance is continued here using the form described in Equation 8, since the integration over $s = [0,+\infty)$ simply requires that the terms a and b be constant in that range.

Substituting Equation 8 into Equation 7 and knowing that the derivative of one is zero, one gets

$$\lambda_{LS} = \int_0^{+\infty} -\frac{d}{ds}\left[\Phi\left(\frac{\ln\theta_C - \ln as^b}{\beta_{DR}}\right)\right] H(s)ds = \int_0^{+\infty} -\frac{d}{ds}\left[\Phi\left(-\frac{\ln s - (\ln\theta_C - \ln a)/b}{\frac{\beta_{DR}}{b}}\right)\right] H(s)ds \tag{9}$$

Given that the CDF is defined in terms of θ, which is a function of s and the derivative in Equation 9 is in terms of s, the chain rule needs to be used. Implementing this cancels the negative sign in front of the derivative and results in the PDF of a lognormal distribution:

$$\lambda_{LS} = \int_0^{+\infty} \frac{b}{\sqrt{2\pi}s\,\beta_{DR}} \exp\left[-\frac{1}{2}\left(\frac{\ln s - (\ln\theta_C - \ln a)/b}{\frac{\beta_{DR}}{b}}\right)^2\right] H(s)ds \tag{10}$$

Recalling that $H(s)$ is defined using a second-order polynomial as in Equation 1, substituting it into Equation 10 gives

$$\lambda_{LS} = \int_0^{+\infty} \frac{k_0 b}{\sqrt{2\pi}s\,\beta_{DR}} \exp\left[-\frac{1}{2}\left(\frac{\ln s - (\ln\theta_C - \ln a)/b}{\frac{\beta_{DR}}{b}}\right)^2 - k_1 \ln s - k_2 \ln^2 s\right] ds \tag{11}$$

As performed by Vamvatsikos,[11] let the term inside the exponential be

$$\begin{aligned}\Delta &= -\frac{1}{2}\left(\frac{\ln s - (\ln\theta_C - \ln a)/b}{\frac{\beta_{DR}}{b}}\right)^2 - k_1 \ln s - k_2 \ln^2 s \\ &= \frac{b^2 \ln s}{\beta_{DR}^2}\left(\underbrace{\frac{(\ln\theta_C - \ln a)}{b} - \frac{k_1\beta_{DR}^2}{b^2}}_{\alpha}\right) - \frac{(\ln\theta_C - \ln a)^2}{2\beta_{DR}^2} - \frac{b^2 \ln^2 s}{2\beta_{DR}^2}\left(\underbrace{1 + \frac{2k_2\beta_{DR}^2}{b^2}}_{1/q}\right)\end{aligned} \tag{12}$$

and let the term inside the first parenthesis be α and the reciprocal of the term inside the second parenthesis be q. Rearranging Equation 12 gives

$$\Delta = \alpha\frac{b^2 \ln s}{\beta_{DR}^2} - \frac{(\ln\theta_C - \ln a)^2}{2\beta_{DR}^2} - \frac{b^2 \ln^2 s}{2q\beta_{DR}^2} \quad = \frac{-b^2(\ln s - \alpha q)^2}{2\beta_{DR}^2 q} + \frac{\alpha^2 q b^2}{2\beta_{DR}^2} - \frac{b^2}{2\beta_{DR}^2}\left(\frac{\ln\theta_C - \ln a}{b}\right)^2 \tag{13}$$

which when substituting back in for α and by letting the logarithm of the intensity at which the capacity is exceeded, s_{θ_c}, be defined by rearranging Equation 8 as per Equation 14:

$$\ln s_{\theta_c} = \frac{\ln\theta_C - \ln a}{b} \tag{14}$$

leads to

$$\Delta = \frac{-b^2}{2\beta_{DR}^2 q}\left(\ln s - q\left(\ln s_{\theta_c} - \frac{k_1\beta_{DR}^2}{b^2}\right)\right)^2 - \frac{b^2}{2\beta_{DR}^2}\left(\ln^2 s_{\theta_c} - q\left(\ln s_{\theta_c} - \frac{k_1\beta_{DR}^2}{b^2}\right)^2\right) \tag{15}$$

Substituting Δ back in Equation 11 gives

$$\lambda_{LS} = \int_0^{+\infty} \frac{k_0 b}{\sqrt{2\pi}s\beta_{DR}} \exp\left[\frac{-b^2}{2\beta_{DR}^2 q}\left(\ln s - q\left(\ln s_{\theta_c} - \frac{k_1\beta_{DR}^2}{b^2}\right)\right)^2 - \frac{b^2}{2\beta_{DR}^2}\left(\ln^2 s_{\theta_c} - q\left(\ln s_{\theta_c} - \frac{k_1\beta_{DR}^2}{b^2}\right)^2\right)\right] ds \tag{16}$$

Multiplying above and below by $\sqrt{q}$ and taking the terms independent of s outside the integral gives

$$\lambda_{LS} = \int_0^{+\infty} \frac{b}{\sqrt{2\pi}s\beta_{DR}\sqrt{q}} \exp\left[-\frac{1}{2}\left(\frac{\ln s - \underbrace{q\left(\ln s_{\theta_c} - \frac{k_1\beta_{DR}^2}{b^2}\right)}_{\mu}}{\underbrace{\frac{\beta_{DR}\sqrt{q}}{b}}_{\sigma}}\right)^2\right] ds \cdot \sqrt{q}k_0 \exp\left[-\frac{b^2}{2\beta_{DR}^2}\left(\ln^2 s_{\theta_c} - q\left(\ln s_{\theta_c} - \frac{k_1\beta_{DR}^2}{b^2}\right)^2\right)\right] \tag{17}$$

where the term inside the integral corresponds to the PDF of a lognormal distribution, $f(\bullet)$, with mean μ and standard deviation σ which by definition is equal to unity when integrated over $s = [0,+\infty)$. Therefore, the integral in Equation 17 could simply be dropped at this point, but is kept in a generalised format for now as

$$\lambda_{LS} = \int_0^{+\infty} f(s)ds \cdot \sqrt{q}k_0 \exp\left[-\frac{b^2}{2\beta_{DR}^2}\left(\ln^2 s_{\theta_c} - q\left(\ln s_{\theta_c} - \frac{k_1\beta_{DR}^2}{b^2}\right)^2\right)\right] \tag{18}$$

By rearranging the terms inside the exponential to a common denominator, expanding out the squared terms and cancelling the common terms, Equation 18 can then be simplified and separated out into

$$\lambda_{LS} = \int_0^{+\infty} f(s)ds \cdot \sqrt{q}k_0 \exp\left[q\left(-k_2 \ln^2 s_{\theta_c} - k_1 \ln s_{\theta_c}\right)\right] \exp\left[\frac{qk_1^2}{2b^2}\beta_{DR}^2\right] \tag{19}$$

By moving the q term in the first exponential term outside by raising to the power of q, then manipulating the k_0 term, the hazard function of the form described in Equation 1 appears for the median capacity intensity, s_{θ_c}, raised to the power of q as follows:

$$\lambda_{LS} = \int_0^{+\infty} f(s)ds \cdot \sqrt{q}k_0^{1-q} H(s_{\theta_c})^q \exp\left[\frac{qk_1^2}{2b^2}\beta_{DR}^2\right] \tag{20}$$

It is noted that capacity, θ_C, has been considered as a deterministic up until this point (ie, $\beta_{CR} = 0$). If it is now considered as a random variable with median, $\widehat{\theta}_C$, and aleatory uncertainty, β_{CR}, its impact can be incorporated into Equation 20 by integrating for all values of θ_C, whilst also assuming that the demand and capacity are independent variables. Vamvatsikos[11] has shown this combination to essentially result in θ_C being replaced by $\widehat{\theta}_C$ and by adding β_{CR}^2 to each of the β_{DR}^2 terms of Equation 20. This derivation is omitted here for brevity, but is noted to result in the following:

$$\lambda_{LS} = \int_0^{+\infty} f(s)ds \cdot \sqrt{\phi}k_0^{1-\phi} H\left(s_{\widehat{\theta}_c}\right)^{\phi} \exp\left[\frac{\phi k_1^2}{2b^2}\left(\beta_{DR}^2 + \beta_{CR}^2\right)\right] \tag{21}$$

where

$$\ln s_{\widehat{\theta}_c} = \frac{\ln \widehat{\theta}_C - \ln a}{b} \tag{22}$$

$$\phi = \frac{1}{1 + \frac{2k_2}{b^2}\left(\beta_{DR}^2 + \beta_{CR}^2\right)} \tag{23}$$

This is essentially a generalised form of the solution presented by Vamvatsikos[11] whereby the integral for intensities is maintained as it will be expanded further in Section 3 to develop the bilinear model.

2.3 | Handling of epistemic uncertainty

The derivation described in Section 2.2 entails three important assumptions regarding the handling of epistemic uncertainty relating to the demand, β_{DU}, capacity, β_{CU}, and hazard, β_{HU}. As outlined by Vamvatsikos,[11] by assuming the hazard to be lognormally distributed with a median value of $\widehat{H}(s)$ and dispersion β_{HU}, to find the mean value, λ_{LS}, the $H(s)^{\phi}$ term in Equations 20 and 21 needs to be substituted with the mean value, $\overline{H(s)^{\phi}}$, which can be approximated by

$$\overline{H(s)^{\phi}} = \left[\widehat{H}(s)\right]^{\phi} \exp\left[0.5\phi^2\beta_{HU}^2\right] \approx \left[\overline{H}(s)\right]^{\phi} \tag{24}$$

where for values of φ close to unity, the mean hazard curve can be used in the above expression. Vamvatsikos[11] then notes that for values $\varphi < 1$, the approximation becomes conservative and suggests that for values of $\varphi < 0.85$, the first form of Equation 24 be used, although the difficulty with this approach is that the median hazard curve and its dispersion are typically not readily available. Acknowledging this assumption and the difficulty created by the format of seismic hazard analysis output formats in implementing the first expansion of Equation 24, the second approximated term is substituted into Equation 21 and used herein. Furthermore, typical values used in Equation 26 are plotted in Figure 3, where it can be seen that this lower bound is generally not exceeded except in extreme cases. Figure 3 provides further illustration of this suggested limit of 0.85 by Vamvatsikos[11] and shows when these aspects of epistemic uncertainty ought to be considered in further detail. Moreover, whilst there is no specific development here in relation to the inclusion of epistemic uncertainty for bilinear demand-intensity model with respect to that of Vamvatsikos,[11] it is still an important aspect to include here given the increasing acknowledgement of the impact of epistemic uncertainties in seismic risk assessment.[21]

Regarding the incorporation of the epistemic uncertainty associated with the demand, β_{DU}, and capacity, β_{CU}, Cornell et al[3] outline how they can be incorporated by assuming that these sources of uncertainty influence the total dispersion only and have no impact on the median values, a common assumption adopted by many past studies for structural response far from collapse.[22-24] This results in the sum of the squares of the epistemic uncertainty being added to the sum of the squares of the aleatory uncertainty already described in Equation 21, to result in

$$\lambda_{LS} = \int_0^{+\infty} f(s)\mathrm{d}s \cdot \sqrt{\phi'} k_0^{1-\phi'} \overline{H}\left(s_{\widehat{\theta_c}}\right)^{\phi'} \exp\left[\frac{\phi' k_1^2}{2b^2}\left(\beta_{DR}^2 + \beta_{CR}^2 + \beta_{DU}^2 + \beta_{CU}^2\right)\right] \tag{25}$$

where

$$\phi' = \frac{1}{1 + \frac{2k_2}{b^2}\left(\beta_{DR}^2 + \beta_{CR}^2 + \beta_{DU}^2 + \beta_{CU}^2\right)} \tag{26}$$

meaning that Equation 25 may be written more succinctly as

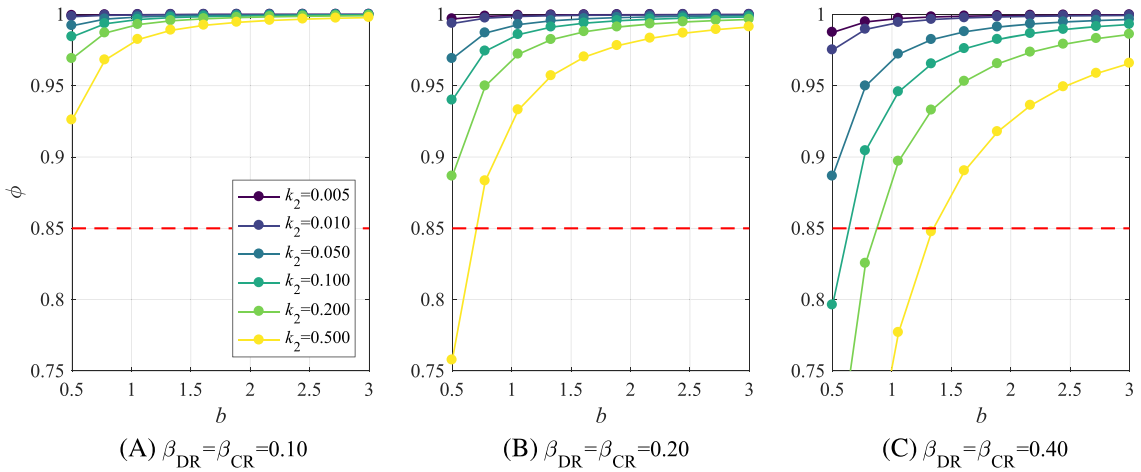

FIGURE 3 Typical values of ϕ for typical values of the demand-intensity model parameter, b, the site hazard curve parameter, k_2, and the dispersion β computed with Equation 26 [Colour figure can be viewed at wileyonlinelibrary.com]

$$\lambda_{\mathrm{LS}} = \int_0^{+\infty} f(s)\mathrm{d}s \cdot G\left(s_{\widehat{\theta}_c}\right) \tag{27}$$

This is essentially a general form of the solution derived by Vamvatsikos[11] for a second-order hazard model fit, whereby the integral of the lognormal PDF on the left-hand side is maintained. It is noted that the above expressions describe the mean estimates of λ_{LS} and user-defined confidence formats such as those outlined in Cornell et al,[3] for example, are not discussed further, but may be developed in future studies.

3 | PROPOSED FORMAT FOR BILINEAR SYSTEMS

The previous section addressed the derivation of a closed-form expression for the MAFE of a given limit state assuming a second-order polynomial fit of the hazard curve and a linear representation of the demand-intensity relationship in logspace. Recalling the different examples outlined in Section 1, where such a demand-intensity model is no longer representative when fitted globally, it is clear that an expansion to the existing linear logspace model is needed for certain structural typologies and demand parameters. These linear logspace models are still adequate when fitted locally to the demand-intensity relationship, but it is often desirable to fit just one single model for ease of application. As such, the generalised form of the expression described in Equation 8 will be taken and further extended to those kinds of structural systems where a single model can be used to describe the demand-intensity relationship over the entire response of the structure. Taking the form of Equation 8 once more, two distinct regions of the demand-intensity model illustrated in Figure 1 are defined as follows:

$$\widehat{\theta}_{\mathrm{D}}(s) \approx \begin{cases} a_1 s^{b_1}, & s < s_{\mathrm{lim}} \\ a_2 s^{b_2}, & s \geq s_{\mathrm{lim}} \end{cases} \tag{28}$$

where s_{lim} is the limiting intensity value at which the linear relationship changes slope in logspace in addition to maintaining its continuity. Since there are two portions to the bilinear model, two pairs of coefficients arise and the term $G(\bullet)$ in Equation 27 becomes as follows:

$$G_1(s) = \sqrt{\phi'_1} k_0^{1-\phi'_1} \overline{H}\left(\widehat{s}_{\theta_c}\right)^{\phi'_1} \exp\left[\frac{k_1^2 \phi'_1}{2b_1^2}\left(\beta_{\mathrm{DR}}^2 + \beta_{\mathrm{CR}}^2 + \beta_{\mathrm{DU}}^2 + \beta_{\mathrm{CU}}^2\right)\right], \quad s < s_{\mathrm{lim}}$$
$$G_2(s) = \sqrt{\phi'_2} k_0^{1-\phi'_2} \overline{H}\left(\widehat{s}_{\theta_c}\right)^{\phi'_2} \exp\left[\frac{k_1^2 \phi'_2}{2b_2^2}\left(\beta_{\mathrm{DR}}^2 + \beta_{\mathrm{CR}}^2 + \beta_{\mathrm{DU}}^2 + \beta_{\mathrm{CU}}^2\right)\right], \quad s \geq s_{\mathrm{lim}} \tag{29}$$

where the $s_{\widehat{\theta}_c}$ are computed from Equation 28 for each range and the corresponding values of ϕ' are described by

$$\phi'_1 = \frac{1}{1 + \frac{2k_2}{b_1^2}\left(\beta_{\mathrm{DR}}^2 + \beta_{\mathrm{CR}}^2 + \beta_{\mathrm{DU}}^2 + \beta_{\mathrm{CU}}^2\right)} \qquad \phi'_2 = \frac{1}{1 + \frac{2k_2}{b_2^2}\left(\beta_{\mathrm{DR}}^2 + \beta_{\mathrm{CR}}^2 + \beta_{\mathrm{DU}}^2 + \beta_{\mathrm{CU}}^2\right)} \tag{30}$$

Although the demand-intensity model formulation in Equation 28 is further distinguished into two zones of median demand with corresponding coefficients, the dispersion values are also assumed to be constant over the entire range of response (ie, homoscedastic). This is an approximation adopted in the initial work by Jalayer[4] for mathematical convenience and also maintained here. A further development of this proposed model may be to consider cases where the dispersion terms in G_1 and G_2 in Equation 29 are not equal but in fact varying with the different zones. However, it is not certain that the actual derivation and practicality of such expressions would be worth the more refined MAFE estimate. These aspects are noted to be a limitation beyond the immediate scope of this work.

Considering the above expansion of the demand-intensity model, Equation 27 is then rewritten as follows:

$$\lambda_{\mathrm{LS}} = \int_0^{s_{\mathrm{lim}}} f_1(\mathrm{s})\mathrm{d}s \cdot G_1\left(s_{\widehat{\theta}_c}\right) + \int_{s_{\mathrm{lim}}}^{+\infty} f_2(\mathrm{s})\mathrm{d}s \cdot G_2\left(s_{\widehat{\theta}_c}\right) \tag{31}$$

where $f_1(s)$ and $f_2(s)$ are the PDFs of a lognormal distribution with mean values of μ_1 and μ_2 and standard deviations of σ_1 and σ_2, respectively, which are given by

$$\mu_1 = \phi'_1\left(\frac{\ln\theta_C - \ln a_1}{b_1} - \frac{k_1\left(\beta_{DR}^2 + \beta_{CR}^2 + \beta_{DU}^2 + \beta_{CU}^2\right)}{b_1^2}\right) \qquad \mu_2 = \phi'_2\left(\frac{\ln\theta_C - \ln a_2}{b_2} - \frac{k_1\left(\beta_{DR}^2 + \beta_{CR}^2 + \beta_{DU}^2 + \beta_{CU}^2\right)}{b_2^2}\right) \tag{32}$$

$$\sigma_1 = \frac{\left(\beta_{DR}^2 + \beta_{CR}^2 + \beta_{DU}^2 + \beta_{CU}^2\right)\sqrt{\phi'_1}}{b_1} \qquad \sigma_2 = \frac{\left(\beta_{DR}^2 + \beta_{CR}^2 + \beta_{DU}^2 + \beta_{CU}^2\right)\sqrt{\phi'_2}}{b_2} \tag{33}$$

Taking Equation 31 and integrating over the specified limits gives the following:

$$\lambda_{LS} = F_1(s_{lim})G_1\left(s_{\widehat{\theta_c}}\right) + [1 - F_2(s_{lim})]G_2\left(s_{\widehat{\theta_c}}\right) \tag{34}$$

where $F_1(s_{lim})$ and $F_2(s_{lim})$ are the CDF values of the corresponding lognormal distributions, described in Equations 32 and 33 above, evaluated at s_{lim}. It is also noted here that whilst the formulation described in Equation 34 has been derived for bilinear demand-intensity models, the same process could be followed for models with additional piecewise linear segments (eg, trilinear) by simply modifying the integration ranges and adding further terms outlined in Equation 31.

It follows that should the coefficients of the two portions of the logspace fit be equal, the above expressions will reduce down to those initially proposed by Vamvatsikos[11] for a second-order hazard fit, and subsequently, should the k_2 term become zero to return to a linear hazard model fit, the above expressions will further reduce down to those initially outlined by Cornell et al.[3] As such, these can be thought of as a further extension and development to the existing framework whereby nonlinear systems whose behaviour with respect to increasing intensity cannot be adequately modelled by a linear fit in logspace over the entire range of response can now be considered. The above expression to compute the MAFE has been implemented in both an Excel spreadsheet and MATLAB script, which can be accessed at the following address: https://github.com/gerardjoreilly/Bilinear-Demand-Intensity.

4 | EXAMPLE APPLICATION

4.1 | Description of structures

To illustrate the application of the proposed extension of performance evaluation solutions for bilinear demand-intensity models, two examples are considered. In specific, these relate to the aforementioned types of situations where a bilinear model is more appropriate than a linear model: the MPSD-intensity relationship in nonductile RC frames with masonry infill and the MPFA-intensity relationship for regular ductile RC frames. Accordingly, two example structures are taken from previous studies and their performance quantified using IDA. The first structure is a three-storey nonductile RC frame with masonry infill described in O'Reilly and Sullivan,[25] numerically modelled as per O'Reilly and Sullivan.[26] The second structure consists of an eight-storey ductile RC frame described by Haselton and Deierlein[27] (building design ID 1011), where the elements were modelled following Haselton et al.[28] Both structures are planar frames and were modelled to include second-order geometry effects and degradation of the structural members.

4.2 | IDA results and demand-intensity model fitting

The case study frames were analysed via IDA with the far-field ground motion set outlined in FEMA P695[29] with the 5% damped first-mode spectral acceleration, $Sa(T_1)$, used to represent the seismic intensity, s. Using the IDA results, the median response and corresponding fractiles were computed through a spline interpolation[30] and are illustrated in Figure 4 in terms of MPSD and MPFA responses of the nonductile and ductile buildings, respectively. In the case of Figure 4A, it can be seen how the IDA curves tend to have a much higher "curvature" as the MPSD increases past θ_{lim}. Figure 4 also shows the limits for each structure that distinguish the two zones of response. In the case of the nonductile RC frame with masonry infills shown in Figure 4A, θ_{lim} was identified as the limiting MPSD equal to 0.18% and corresponding to the peak force of the masonry infills, as previously identified by O'Reilly.[17] For the ductile RC frame shown in Figure 4B, the limiting intensity, s_{lim}, was determined as 0.17 g by transforming the base shear at yield identified from pushover analysis to a yield spectral acceleration for the structure. From these IDA results, characterised by the median response with respect to increasing intensity, the demand-intensity models can be identified for each structure. This is illustrated in Figure 5, whereby the IDA results are plotted in logspace. It is clear in both cases that when compared

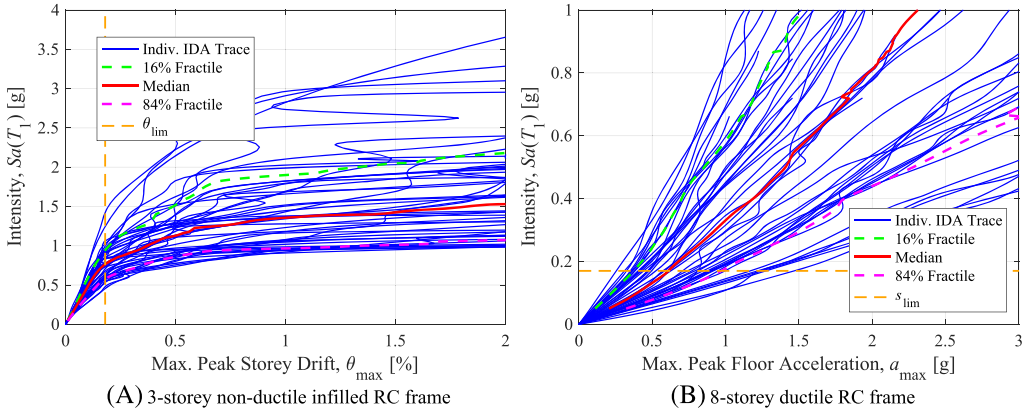

FIGURE 4 IDA results for each individual ground motion, together with the median response and 16% and 84% fractiles, for the two case study structures examined [Colour figure can be viewed at wileyonlinelibrary.com]

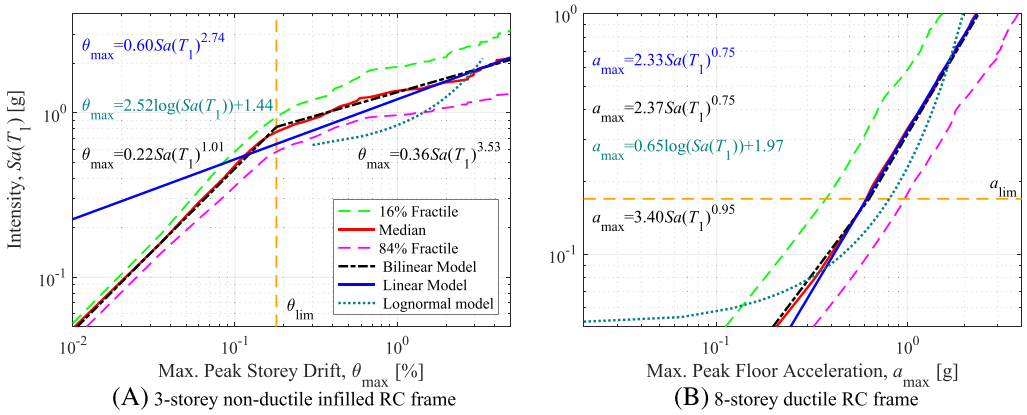

FIGURE 5 IDA results characterised by the median response and 16% and 84% fractiles plotted in logspace for two case study structures, where the various demand-intensity models discussed thus far are illustrated along with their function forms and fitted coefficients [Colour figure can be viewed at wileyonlinelibrary.com]

with the limiting demand intensities in Figure 5A and 5B, respectively, two distinct zones of response can be identified for the structural response.

To demonstrate the impacts of the proposed expressions in Section 3, a number of approaches were adopted to estimate the MAFE of a given limit state:

- Global fit—linear model: The linear model described by Equation 8 was fitted globally over the entire range of structural response and is represented by the blue lines in Figure 5.
- Global fit—bilinear model: The bilinear model developed in Section 3 and described by Equation 28 was fitted for the two zones of response previously described and is illustrated via the black lines in Figure 5. Care was taken to ensure that the fitted coefficients resulted in a continuous bilinear model over the entire range of response and did not exhibit any discontinuity at the limiting interface.
- Local fit—linear model: The models fitted locally in both zones of response for the first approach above are used over the entire range of response to examine whether simply using a local fit in each of the respective zones would be sufficient in certain cases. This essentially implies that instead of using the weighting combinations of G_1 and G_2 described in Equation 34, these individual functions are used over the entire range of response.

The logarithmic functional form proposed by Romão et al[12] was also fitted to the median response of both structures. From Figure 5A, it is clear that this model is not representative of the MPSD demand in infilled RC frames, which was anticipated due to the inversion of the dependent and independent variables chosen by Romão et al,[12] meaning that the unsatisfactory fit shown in Figure 5A is an expected result. It is noted, however, that when these variables were reversed in the logarithmic function (ie, switching $Sa(T_1)$ and θ_{max}), the fitting to the median demand shown in Figure 6 is quite

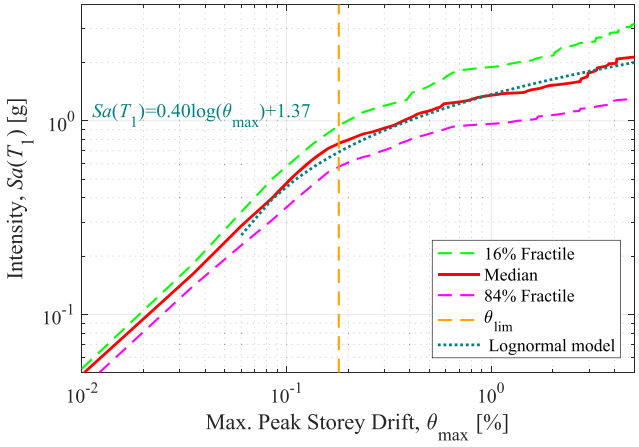

FIGURE 6 Fitting of the lognormal model proposed by Romão et al[12] to the median MPSD demand in the three-storey nonductile RC frame when the terms are switched [Colour figure can be viewed at wileyonlinelibrary.com]

good. Therefore, should such a logarithmic function be derived again in this form, it may be expected to be much improved. For the case of the MPFA, Figure 5B shows how the logarithmic function is not very representative of the demand-intensity relationship and the bilinear fit appears more favourable. This is identified as one of the benefits of the bilinear model, where the dynamic characteristics can be separated into two zones of response and fitted to accordingly, as opposed to forcing a single functional form over the entire response.

For each model discussed above, their respective coefficients were fitted using least squares regression to the median values plotted in Figure 4 and are illustrated in Figure 5 with the coefficients printed using the same colour. For the purposes of illustration, the hazard model coefficients outlined in Equation 1 were taken as $k_0 = 7 \times 10^{-4}$, $k_1 = 2.0$, and $k_2 = 0.30$ for both structures using values from a site in Italy of moderate seismicity discussed in O'Reilly et al[31] as a reference point to give reasonable values. It is acknowledged that these coefficients would be expected to differ for the two structures due to the difference in fundamental period, but this simplification will have no impact on the conclusions presented herein since the results are presented relative to one another for each structure individually.

4.3 | Performance evaluation results and discussion

Using the demand-intensity models shown in Figure 5, the MAFE for increasing demand was calculated. For each fit, a number of approaches were adopted to compute the MAFE illustrated in Figure 7 and are described as follows:

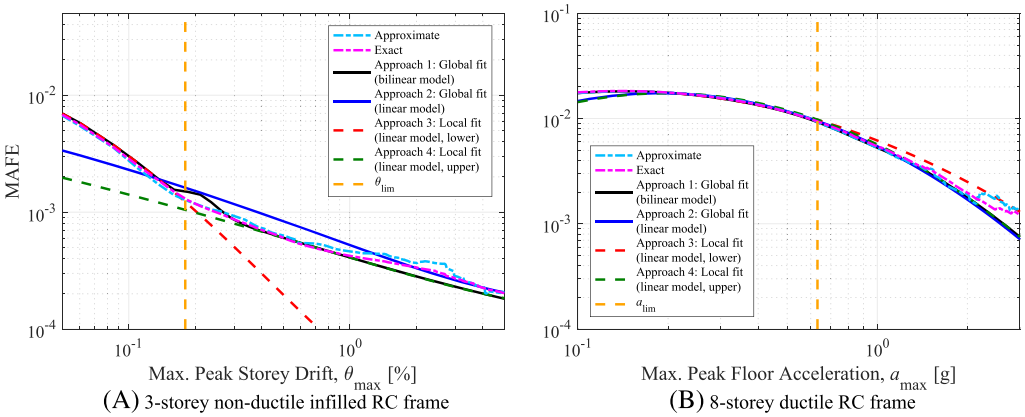

FIGURE 7 Comparison of the MAFE estimates for each approach, where the approximate and exact values computed directly from the IDA results are shown for comparison and evaluation [Colour figure can be viewed at wileyonlinelibrary.com]

- Approximate: For a given value of demand, the MAFE was approximated by taking a vertical slice in the IDA curves shown in Figure 4 and noting the intensities at which each individual ground motion trace exceeds this given level of demand. Using these intensity values, a lognormal distribution was fitted and the MAFE computed using the intensity-based MAFE formulation described in Vamvatsikos[11] with the hazard parameters outlined previously. This is termed "approximate" here as it relies on the assumption of lognormality of the data.
- Exact: Contrary to the *approximate* estimation above, the "exact" value of MAFE was obtained by taking these same intensities at which a given demand is exceeded for each IDA trace, computing their empirical cumulative distribution function and directly integrating with the hazard to get the MAFE via Equation 5. Since it is a direct integration of the IDA results, it does not require a lognormal distribution to be fitted.
- Approach 1: The global fit of the bilinear model illustrated in Figure 5 was utilised with the expressions outlined in Section 3 to evaluate the MAFE at increasing levels of demand, which is the model being proposed.
- Approach 2: The global fit of the linear model shown in Figure 5 was used with the demand-based formulation of the SAC/FEMA expressions extended in Vamvatsikos[11] for a second-order hazard model.
- Approach 3: The local fit of the linear model for the lower region was used in combination with the demand-based expressions to estimate the MAFE,[11] where the lower region denotes the region beneath the limiting threshold values (ie, θ_{lim} or a_{lim}) illustrated in Figure 7.
- Approach 4: This is the same implementation as approach 3 but is for the local fit of the linear model in the upper region as opposed to the lower region.

Each of these approaches was used and compared with the values obtained from the exact integration of the IDA results. Since the exact integration of the results considers only record-to-record variability, the epistemic uncertainty terms, β_{DU} and β_{CU}, were set to zero in order to maintain consistency. Additionally, since the dispersion due to record-to-record variability in Figure 4 was estimated from the IDA fractiles using the approximate method, these dispersions were used directly in the intensity-based formulation for MAFE. For the demand-based formulation, the intensity-based dispersions were converted via the demand-intensity relationship parameter b, since it can be easily shown that demand-based and intensity-based measures of dispersion are related through this parameter.

Examining the comparison between the exact and approximate estimates of MAFE for increasing demand, there is a reasonably good match for both case study structures. Some discrepancy is noted due to the assumption of lognormality of the data breaking down in some instances, but the overall matching is quite good. Comparing the use of the different linear models (approaches 2 to 4) with the integrated results shows a number of interesting observations. First, the local fits (approaches 3 and 4) match the MAFE computed from direct integration very well in their respective regions of fitting, but are noted to grossly underestimate the MAFE outside of these regions in Figure 7A and tend to slightly overestimate for approach 3 in Figure 7B beyond the threshold of a_{lim}. It is noted that the MAFE for each approach in Figure 7B slightly reduces for decreasing MPFA when it would be anticipated to flatten out and approach the baseline rate of hazard for low-intensity levels. This is just a consequence of the inherent curvature of the hazard formulation resulting from the fitting parameters chosen here (ie, k_0, k_1, and k_2) whose exceedance rate reduces instead of stabilises for very low intensity levels. Should the adopted hazard parameters be fitted well to the hazard data over all intensity levels, this reduction seen in Figure 7B should no longer be presented. In the case of the linear model fitted globally (approach 2), this can be seen to completely misrepresent the MAFE at all demand levels for both structures. This is a somewhat expected result as the fitting of this model was not optimal even when evaluating Figure 5 visually. As a result, it can be stated that the use of a global fit of a linear model cannot be reasonably used for such structures, but local fits can be utilised in their respective zones of fitting provided they are sufficiently far from the transition point, which is further discussed below. For the proposed bilinear demand-intensity model (approach 1), the comparison with the direct integration results is very promising for the case of both MPSD and MPFA exceedance shown in Figure 7. This is seen by how it gradually shifts from the estimates of the locals fits across the transition point to give a single demand-intensity model that can accurately assess the MAFE across the entire region of response. Some discrepancy is noted at a few locations but is deemed to be as a result of the estimation of demand-based dispersion in addition to the inherent error of the fit and simplified approximation.

It is important to note that the typical level of dispersion associated with such models was somewhat underrepresented in Figure 7, where the epistemic uncertainty was maintained at zero in order to provide a meaningful comparison with the IDA results. This is a key point to note with respect to the proposed model as the closer the demand value of interest is to the transition point and the higher the overall uncertainty is, the more unreliable the local fits of the linear model will become since there is no longer a continuous projection of the local demand to intensity, as illustrated

in Figure 8. It therefore means that a zone around the transition point exists, inside which local fits may no longer be used and the proposed bilinear should be used. Such a zone may be seen in Figure 7A, where a gradual transition of the MAFE computed via direct integration was observed whereas the local linear models gave an abrupt transition. To illustrate this aspect further, a relative comparison between the local fits examined in Figure 7A is performed. The same fitting coefficients are maintained, but the dispersion, however, is modified to highlight its impact. From the expressions outlined in Section 3, the total dispersion, β_{TOT}, is defined here as the square root sum of the squares of the β terms in Equation 25. Repeating the above calculations for a range of β_{TOT} values and expressing as a ratio to the proposed bilinear model, Figure 9 below shows the impact the uncertainty has on the usefulness of the local fits in the vicinity of the transition point. It can be seen how the greater the dispersion, the greater the error is when estimating the MAFE is using the local fit models with respect to the proposed bilinear model. For the case of no dispersion, the ratios are maintained at unity for the lower fit (solid black line) and upper fit (dashed black line) to the left and right of the drift limit, respectively, but are seen to quickly become unconservative (ie, they under predict the MAFE) beyond this limit. As the dispersion is increased, the local fits begin to lose their fidelity with respect to the bilinear model, especially to the right of the transition point.

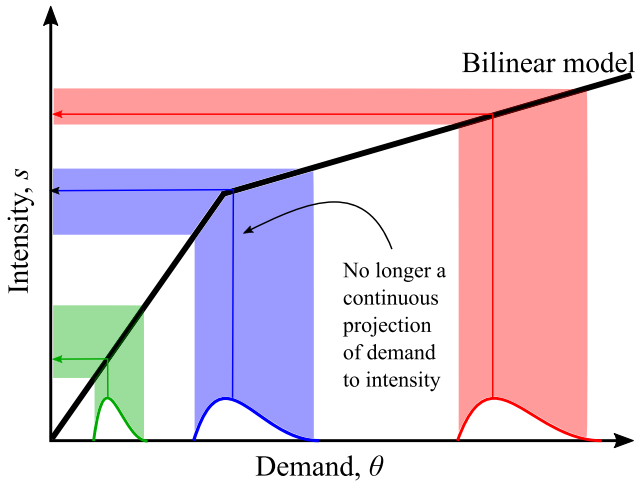

FIGURE 8 Illustration of the projection using a demand-intensity model, where for demands far away from the limiting interface (green and red), there is a continuous projection of the demand using the local fit, but when the demand is close to the interface (blue), it becomes discontinuous [Colour figure can be viewed at wileyonlinelibrary.com]

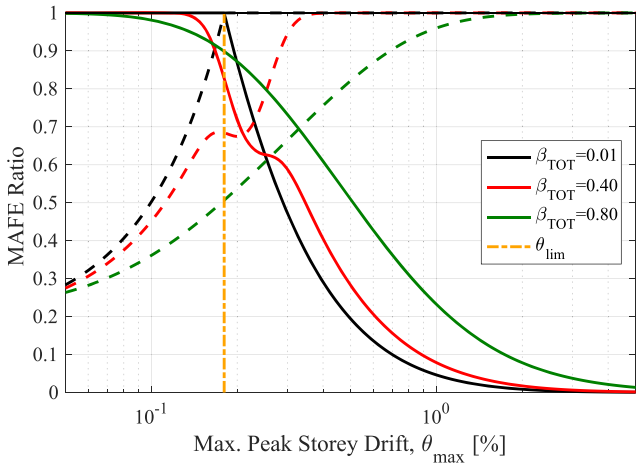

FIGURE 9 Impact of the total uncertainty, β_{TOT}, on the use of local fits of a linear demand-intensity model to compute MAFE, where approach 3 (solid lines) and approach 4 (dashed lines) are expressed as ratio to the bilinear model (approach 2) and work well to the left and right of the limiting threshold, respectively, for low levels of dispersion [Colour figure can be viewed at wileyonlinelibrary.com]

For the evaluation of drift demand well into the nonlinear range of response, this would not be expected to be problematic, as described in Figure 8. However, in the case of MPSD demand shown in Figure 9, it can be seen how the local fits are not reasonable to adopt with the region of 0.15% to 0.70% for $\beta_{TOT} = 0.80$ as the difference to the bilinear model is over 10%, which would correspond to the range of MPSD demand typically associated with nonstructural component damage and structural yielding in the case of infilled RC frames. Therefore, it is critical that the performance of such structures be represented adequately via an appropriate demand-intensity model when computing the MAFE in closed-form so as not to misrepresent their exceedance rates, as Figures 7 and 9 have demonstrated.

5 | SUMMARY

An extension to the existing SAC/FEMA closed-form expressions has been developed here, whereby structural systems whose median demand-intensity relationship cannot be reasonably represented via a single linear fit in logspace, but rather a bilinear fit, may now be considered. The derivation of the expressions was outlined in resonance with previous studies on the matter to clearly illustrate the extension to the existing framework being proposed here. Different aspects were examined, and an example application was presented for two different situations where the model developed here is required. Specifically, the characterisation of peak storey drift with increasing spectral acceleration for nonductile RC frames with masonry infill and the characterisation of peak floor acceleration with increasing spectral acceleration for ductile RC frames were addressed. This example application illustrated that, in terms of mean annual frequency of exceedance (MAFE), local fitting of the demand-intensity model in the respective zones of structural response was a reasonable approximation up until a certain point. It was shown that as long as the demand was far enough away from the interface between the two zones of response, the use of a locally fitted model was reasonable. However, as the demand became closer to the limiting demand, the discontinuous projection of the demand to intensity required the individual integration with these two segregated zones of response with the hazard curve, in order to more accurately compute the MAFE. It was also shown that using a global fit of a linear model over the entire range of response was not applicable at all for such cases. Lastly, it was shown that although the logarithmic demand-intensity model for force-based parameters is a worthwhile development, it was not applicable in the specific cases discussed here. Still, it was noted as having the potential to be extended as part of future work.

Overall, this work represents a novel contribution to the existing framework for performance-based evaluation of structural systems characterised by a bilinear demand-intensity relationship, where the unique case of equal coefficients in both zones simply means that the proposed solution simplifies back into the existing framework. It may also be further extended to other piecewise linear demand-intensity formulations such as trilinear models by simply modifying the integration ranges and adding further terms to Equation 34. Another future development that has not been incorporated here is for the extension of these expressions to incorporate a confidence-based format, similar to that outlined by Cornell et al,[3] among others.

ACKNOWLEDGEMENTS

The work presented in this paper has been developed within the framework of the project "Dipartimenti di Eccellenza", funded by the Italian Ministry of Education, University and Research at IUSS Pavia. The first author also acknowledges the many fruitful discussions with Athanasios Papadopoulos regarding different aspects relating to Section 2. The authors would also like to thank Prof. Dimitrios Vamvatsikos and Prof. Carmine Galasso for their valuable comments and suggestions.

ORCID

Gerard J. O'Reilly http://orcid.org/0000-0001-5497-030X
Ricardo Monteiro http://orcid.org/0000-0002-2505-2996

REFERENCES

1. SEAOC. *Vision 2000: Performance-Based Seismic Engineering of Buildings*. Sacramento: California; 1995.

2. Cornell CA, Krawinkler H. Progress and challenges in seismic performance assessment. PEER Center News 2000; 3(2): 1–2.

3. Cornell CA, Jalayer F, Hamburger RO, Foutch DA. Probabilistic basis for 2000 SAC Federal Emergency Management Agency steel moment frame guidelines. *Journal of Structural Engineering*. 2002;128(4):526-533. https://doi.org/10.1061/(ASCE)0733-9445(2002)128:4(526).
4. Jalayer F. Direct probabilistic seismic analysis: implementing non-linear dynamic assessments. PhD Thesis, Stanford University, *USA*, 2003.
5. Lupoi G, Lupoi A, Pinto PE. Seismic risk assessment of RC structures with the "2000 SAC/FEMA" method. *Journal of Earthquake Engineering*. 2002;6(4):499-512. https://doi.org/10.1080/13632460209350427
6. Welch DP, Sullivan TJ, Calvi GM. Developing direct displacement-based procedures for simplified loss assessment in performance-based earthquake engineering. *Journal of Earthquake Engineering*. 2014;18(2):290-322. https://doi.org/10.1080/13632469.2013.851046
7. Fajfar P, Dolšek M. A practice-oriented estimation of the failure probability of building structures. *Earthquake Engineering & Structural Dynamics*. 2012;41(3):531-547. https://doi.org/10.1002/eqe.1143
8. Franchin P, Pinto PE. Method for probabilistic displacement-based design of RC structures. *Journal of Structural Engineering*. 2012;138(5):585-591. https://doi.org/10.1061/(ASCE)ST.1943-541X.0000492
9. Vamvatsikos D, Aschheim MA. Performance-based seismic design via yield frequency spectra. *Earthquake Engineering & Structural Dynamics*. 2016;45(11):1759-1778. https://doi.org/10.1002/eqe.2727
10. CNR. Istruzioni per la Valutazione Affidabilistica della Sicurezza Sismica di Edifici Esistenti. CNR – Commissione Di Studio per La Predisposizione e l'analisi Di Norme Tecniche Relative Alle Costruzioni 2014.
11. Vamvatsikos D. Derivation of new SAC/FEMA performance evaluation solutions with second-order hazard approximation. *Earthquake Engineering & Structural Dynamics*. 2013;42(8):1171-1188. https://doi.org/10.1002/eqe.2265
12. Romão X, Delgado R, Costa A. Alternative closed-form solutions for the mean rate of exceedance of structural limit states. *Earthquake Engineering & Structural Dynamics*. 2013;42(12):1827-1845. https://doi.org/10.1002/eqe.2300
13. Vamvatsikos D, Cornell CA. Incremental dynamic analysis. *Earthquake Engineering & Structural Dynamics*. 2002;31(3):491-514. https://doi.org/10.1002/eqe.141
14. Sullivan TJ, Saborío-Romano D, O'Reilly GJ, Welch DP, Landi L. Simplified pushover analysis of moment resisting frame structures. Submitted to *Journal of Earthquake Engineering* 2018. https://doi.org/10.1080/13632469.2018.1528911
15. Stillmaker K, Lao X, Galasso C, Kanvinde A. Column splice fracture effects on the seismic performance of steel moment frames. *J Constr Steel Res*. 2017;137(June):93-101. https://doi.org/10.1016/j.jcsr.2017.06.013
16. Galasso C, Stillmaker K, Eltit C, Kanvinde A. Probabilistic demand and fragility assessment of welded column splices in steel moment frames. *Earthquake Engineering & Structural Dynamics*. 2015;44(11):1823-1840. https://doi.org/10.1002/eqe.2557
17. O'Reilly GJ. Performance-based seismic assessment and retrofit of existing RC frame buildings in Italy. PhD Thesis, IUSS Pavia, Italy, 2016.
18. Ramamoorthy SK, Gardoni P, Bracci JM. Probabilistic demand models and fragility curves for reinforced concrete frames. *Journal of Structural Engineering*. 2006;132(10):1563-1572. https://doi.org/10.1061/(ASCE)0733-9445(2006)132:10(1563).
19. NIST. Applicability of nonlinear multiple-degree-of-freedom modeling for design. NIST GCR 10–917-9 2010: 1–222.
20. Aslani H, Miranda E. Probability-based seismic response analysis. *Eng Struct*. 2005;27(8):1151-1163. https://doi.org/10.1016/j.engstruct.2005.02.015
21. Bradley BA. A critical examination of seismic response uncertainty analysis in earthquake engineering. *Earthquake Engineering & Structural Dynamics*. 2013;42(11):1717-1729. https://doi.org/10.1002/eqe.2331
22. Dolšek M. Incremental dynamic analysis with consideration of modeling uncertainties. *Earthquake Engineering and Structural Dynamics*. 2009;38(6):805-825. https://doi.org/10.1002/eqe.869
23. Vamvatsikos D, Fragiadakis M. Incremental dynamic analysis for estimating seismic performance sensitivity and uncertainty. *Earthquake Engineering & Structural Dynamics*. 2010;39(2):141-163. https://doi.org/10.1002/eqe.935.
24. O'Reilly GJ, Sullivan TJ. Quantification of modelling uncertainty in existing Italian RC frames. *Earthquake Engineering & Structural Dynamics*. 2018;47(4):1054-1074. https://doi.org/10.1002/eqe.3005
25. O'Reilly GJ, Sullivan TJ. Probabilistic seismic assessment and retrofit considerations for Italian RC frame buildings. *Bulletin of Earthquake Engineering*. 2018;16(3):1447-1485. https://doi.org/10.1007/s10518-017-0257-9
26. O'Reilly GJ, Sullivan TJ. Modeling techniques for the seismic assessment of the existing Italian RC frame structures. *Journal of Earthquake Engineering*. 2017;1-35. https://doi.org/10.1080/13632469.2017.1360224
27. Haselton CB, Deierlein GG. Assessing seismic collapse of modern reinforced concrete moment frame buildings. Blume Report no 156 2007.
28. Haselton CB, Liel AB, Taylor Lange S, Deierlein GG. Beam-column element model calibrated for predicting flexural response leading to global collapse of RC frame buildings. PEER Report 2007/03 2008.
29. FEMA P695s. *Quantification of Building Seismic Performance Factors*. Washington, DC, USA; 2009.

30. Vamvatsikos D, Cornell CA. Applied incremental dynamic analysis. *Earthq Spectra*. 2004;20(2):523-553. https://doi.org/10.1193/1.1737737

31. O'Reilly GJ, Perrone D, Fox M, Monteiro R, Filiatrault A. Seismic assessment and loss estimation of existing school buildings in Italy. *Eng Struct*. 2018;168:142-162. https://doi.org/10.1016/j.engstruct.2018.04.056

How to cite this article: O'Reilly GJ, Monteiro R. Probabilistic models for structures with bilinear demand-intensity relationships. *Earthquake Engng Struct Dyn*. 2018;1–16. https://doi.org/10.1002/eqe.3135